Hyperfine Fields of sp Impurities on Ni and Fe Surfaces

Ph. Mavropoulos and N. Stefanou
Section of Solid State Physics, University of Athens, Panepistimioupolis, GR-157 84 Athens, Greece

B. Nonas, R. Zeller, and P. H. Dederichs
Institut für Festkörperforschung, Forschungszentrum Jülich, D-52425 Jülich, Germany
(Received 15 May 1998)

We present first-principles calculations of the electronic structure and hyperfine fields of $4sp$ impurities on the (001) surfaces of Ni and Fe. The calculations are based on the local-spin-density-functional theory and employ a Green's function method for impurities at surfaces. The systematic behavior obtained for the hyperfine fields of adatoms or impurities in the first surface layer is completely different from that found in the bulk, mainly due to the reduction of the symmetry and the coordination number at the surface. Our results explain the surprisingly small hyperfine-field values measured for Se adatoms and provide challenging predictions to be confirmed by future experiments. [S0031-9007(98)06862-8]

PACS numbers: 75.30.Pd, 73.20.Hb, 76.60.Jx

Hyperfine-interaction measurements provide unique information about the electronic properties of solids which cannot be obtained by other methods. However, since this information originates from the inner region of the atoms close to the nucleus, it is in general difficult to understand and interpret. In ferromagnetic materials such as Fe, Co, Ni, and their alloys, the hyperfine field H_{hf} is the most important hyperfine quantity that is directly related to the magnetization density at the nucleus. In the past. numerous experiments have been performed for impurities extending more or less across the whole periodic table [1]. A theoretical explanation of the systematic variation of the impurity hyperfine fields as a function of the atomic number of the impurity has been first given by Kanamori *et al.* [2] and subsequently confirmed by *ab initio* calculations [3–5]. According to this, for sp impurities, the negative hyperfine fields at the beginning of an sp series arise from bonding s-d hybrids, which show a preferential occupation of the minority-spin states. On the other hand, the strong increase to large positive hyperfine-field values at the end of the sp series and the abrupt decrease to negative values at the beginning of the next row of the periodic table are due to the occupation of the spin-split antibonding states close to the Fermi level E_F.

In recent years, interesting hyperfine-field measurements have been performed using the perturbed-angular-correlation (PAC) technique with probe atoms at surfaces and interfaces, in order to investigate the complicated electronic and magnetic properties of these systems [6–9]. While in earlier works the ^{111}In/^{111}Cd probe has been used, the availability of the ISOLDE mass separator at CERN also allowed the study of more exotic systems such as, e.g., ^{77}Br nuclei decaying into ^{77}Se. Granzer *et al.* [7] have used this probe in recent PAC experiments for Se on the Ni(001) and (111) surfaces, where Br and Se are known to occupy adatom positions [10]. While in bulk Ni the Se impurity has a hyperfine field of about 150 kG [11], Granzer *et al.* found the surprising result that the Se adatom shows a very small hyperfine field: 8 kG on the (001) and 27 kG on the (111) surface of Ni.

Motivated by these puzzling findings, we have carried out a systematic *ab initio* study of the hyperfine field for a complete series of sp impurities on the (001) surfaces of fcc Ni and bcc Fe, as well as in bulk Ni and Fe. In particular, we consider the impurities of the $4sp$ series, starting from Cu and Zn, up to Rb and Sr in the next series, and we investigate three different positions of the impurity atoms: (i) in the bulk, (ii) on top of the surface as an adatom (fourfold hollow site), and (iii) in the surface layer by substituting a substrate atom (terrace position).

Our calculations are based on density-functional theory in the local-spin-density approximation (LSDA) and employ the Korringa-Kohn-Rostoker (KKR) Green's function method for defects at surfaces [12] or in bulk crystals [13]. Multiple-scattering theory is applied to obtain the Green's function in angular-momentum representation from an algebraic Dyson equation given by

$$G_{LL'}^{nn'} = G_{LL'}^{0\,nn'} + \sum_{n'',L''} G_{LL''}^{0\,nn''} \Delta t_{L''}^{n''} G_{L''L'}^{n''n'}, \qquad (1)$$

where $G_{LL'}^{nn'}(E)$ denotes the energy-dependent structural Green's function matrix elements and $G_{LL'}^{0\,nn'}(E)$ denotes the corresponding matrix elements for the host medium (ideal infinite or semi-infinite crystal) which serves as a reference system. The summation in Eq. (1) runs over all lattice sites n'' and angular-momentum quantum numbers $L'' = \{\ell'' m''\}$ for which the perturbation $\Delta t_{L''}^{n''}(E) = t_{L''}^{n''}(E) - t_{L''}^{0\,n''}(E)$ of the t matrix between the defect and the reference system is significant. In the calculations we include angular momenta up to $\ell = 3$. While we assume the impurity and its first 12 nearest-neighbor cells to be perturbed for the fcc structure (Ni), in the case of the bcc structure (Fe) we take into account more than two

perturbed shells of neighbor potentials, in order to ensure adequate convergence. The site-centered potentials are considered in the atomic-sphere approximation, i.e., they are assumed to be spherically symmetric around the proper atomic center and nonvanishing within a sphere of atomic volume. However, the full nonspherical charge density is calculated at each iteration step of the self-consistency procedure by taking angular momenta up to $\ell = 6$ into account in the multipole expansion. Exchange and correlation effects are included in the LSDA using the parametrization of Vosko *et al.* [14]. The calculations are performed in the scalar-relativistic approximation [15]. Further on, we neglect lattice relaxations, which should not seriously affect our conclusions since the trends of the hyperfine fields are more or less independent of moderate lattice distortions.

In the cases we examined, the dominant contribution to the hyperfine field is given by the Fermi contact interaction which, in the nonrelativistic limit, has the following form: $H_{\rm hf} = \frac{8\pi}{3} m(\mathbf{r} = 0)$. We note that the magnetization density at the nucleus, $m(\mathbf{r} = 0)$, is determined by the s electrons only. In a relativistic treatment, as done in the present paper, Breit's formula has to be used instead of the Fermi contact term [4,5]. In line with the scalar-relativistic approximation, orbital contributions to the hyperfine field are neglected, and the same applies to the dipolar field contributions, both of which are expected to lead to only minor corrections of the present results.

Figure 1 shows our results for the hyperfine fields of the $4sp$ impurities on the Ni(001) surface, as well as in bulk Ni. Our calculations show that the hyperfine field is essentially determined from the polarization of the s valence states of the impurity, while the core-electron contributions are negligibly small in all of the cases examined, as expected for nonmagnetic impurities. We note that the valence contribution to the hyperfine field can be more or less linearly scaled to the s magnetic moment of the impurity.

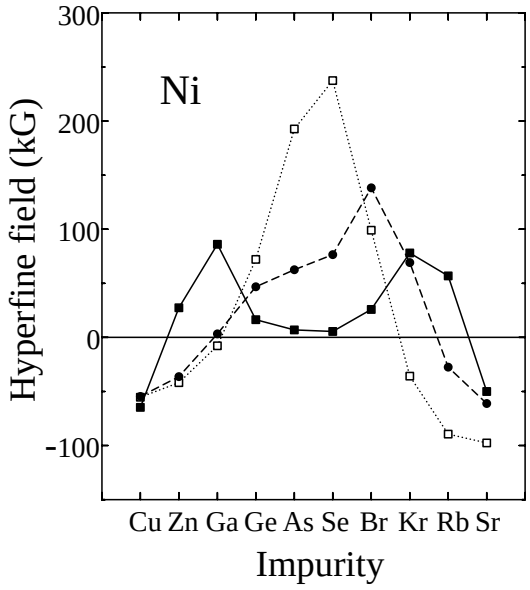

FIG. 1. Hyperfine field of sp impurities in bulk Ni (open squares, dotted line), in the first surface layer of Ni(001) (solid circles, dashed line), and adsorbed on Ni(001) (solid squares, solid line).

In bulk Ni (Fig. 1, dotted line) the hyperfine field is negative for Cu and Zn, it increases and takes its maximum value at Se, and then decreases abruptly taking negative values at the beginning of the next $(5sp)$ series. As explained by Kanamori *et al.* [2] the maximum occurs due to the preferential filling of s-like antibonding states in the majority-spin band, while the subsequent filling of the antibonding states in the minority-spin band leads to the fast decrease of the hyperfine fields for Br and Kr impurities. The progressive filling of the impurity s states is illustrated in Fig. 2 (right side) which shows the s-projected local density of states (LDOS) for Ga, Se, and Kr impurities in bulk Ni. Since the difference in the population of the antibonding states between majority- and minority-spin bands becomes largest for Se, one obtains in this case the largest positive s magnetic moment which explains the very high hyperfine-field value of the Se impurity.

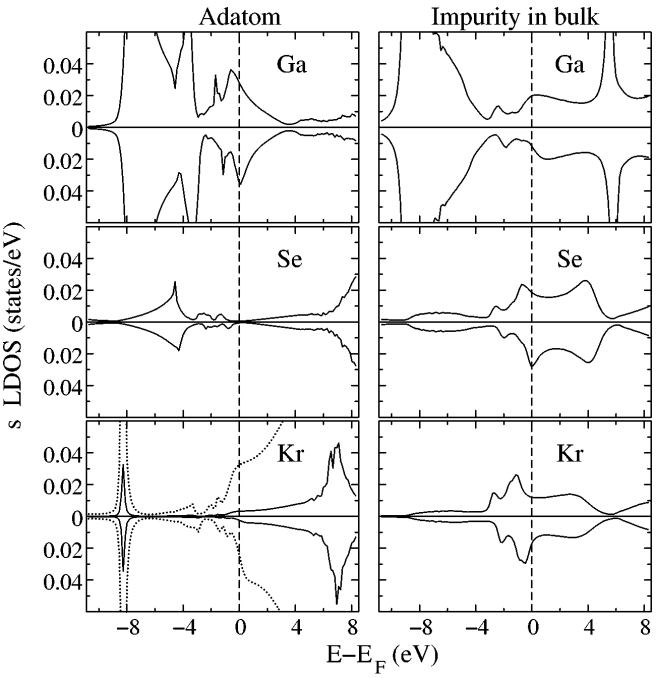

FIG. 2. Spin-resolved s LDOS of Ga, Ge, and Kr adatoms on Ni(001) (left), and impurities in bulk Ni (right). The upper (lower) parts of the figure correspond to the majority (minority)-spin states. In the adatom case, the first antibonding peak crosses the Fermi level for Ga, while the second is higher up, above 4 eV. For Se, E_F separates the two antibonding peaks, and for Kr the second antibonding state crosses E_F while the $5s$ state appears at about 7 eV (the dotted line represents a magnification by a factor of 10). In the case of impurities in bulk, the (one and only) antibonding peak is always situated near the Fermi level.

The situation is, however, very different for the adatoms. Here the hyperfine field shows two peaks (see Fig. 1). The first peak already occurs at Ga and the second one at Kr, with a pronounced valley of small field values for the intermediate elements Ge, As, Se, and Br. Negative hyperfine fields are obtained only for Cu and Sr. The behavior of the impurities in the first surface layer is intermediate between the adatom and bulk cases. Here the first maximum develops into a broader shoulder and the second maximum is increased and shifted to smaller valences. The calculated hyperfine field of 5.5 kG for the Se adatom is in very good agreement with a recent experiment [7] which yields 8 ± 3 kG. Both values are in sharp contrast to the large field obtained for a Se impurity in bulk Ni.

As we observe in Fig. 1, H_{hf} increases versus the impurity atomic number at the beginning of the sp series and takes a maximum value at a smaller atomic number for the adatoms than for impurities in bulk. This is due to the reduced coordination number and the resulting smaller bonding-antibonding splitting of the impurity s states at the surface, as can be seen by comparing the left and right sides of Fig. 2 for the Ga impurities.

Because of the reduced symmetry (C_{4v}) at the (001) surfaces of Ni and Fe as compared with the bulk, the hybridization of the s and p impurity states with the $3d$ orbitals of the substrate results in the formation of on-site s-p_z hybrids. This can occur because both the s and p_z impurity orbitals transform according to the same irreducible representation (the identity representation) of the point symmetry group C_{4v}, which is not the case in the bulk, where s and p orbitals transform according to different irreducible representations of the point symmetry group O_h. Therefore, for the impurities at surfaces, we can understand the features of the s LDOS (see Fig. 2, left side) by considering the hybridization between each of the two s-p_z impurity hybrids ($\approx|s\rangle \pm |p_z\rangle$) and the d states of the neighboring host atoms. This explains why we obtain a doubling of the s-like bonding and antibonding peaks, as can be seen by comparing the left and right sides of Fig. 2. The s-p_z impurity hybrid which is directed towards the substrate hybridizes more strongly with the host d states than the hybrid which points to the opposite direction, due to the larger spatial overlap. This difference in the hybridization strength gives rise to two antibonding s peaks separated by a region of vanishingly small LDOS, for each spin direction. As can be seen from Fig. 2, in the case of a Ga adatom the first s antibonding peak for each spin direction crosses E_F, while, for Se, E_F lies in the valley of the s LDOS and, for Kr, E_F is situated in the region of the second antibonding peak. The s-p_z hybridization can also be seen in the peak of the Kr s-LDOS at -8 eV, which represents a parasite of the localized $4p_z$ level, situated at this energy.

The above considerations imply the following physical picture for the progressive filling of the antibonding s states as we move along the series from Cu to Sr. For impurities in the bulk, these antibonding states form a relatively broad peak of low intensity for each spin direction. Spin-up states are initially filled more rapidly than the spin-down states, since they are lower in energy. Thus, the s impurity moment and the hyperfine field increase and take their largest values at Se. Then, the filling of the spin-down antibonding states and partly also of the bonding $5s$ states (the latter yield a negative spin polarization [2,3,5]) decreases the s moment and the hyperfine field which become negative for Kr, Rb, and Sr. On the other hand, in the case of adatoms, for each spin direction, the s antibonding states form a first peak followed by an energy region almost empty of states and then a second peak of low but nonvanishing intensity. First are filled the spin-up states of the first peak, giving a positive contribution to the s moment and the hyperfine field which reach a maximum at Ga. Subsequently, the filling of the corresponding spin-down states cancels this polarization, which becomes vanishingly small for As and Se. As we move to the next elements, the same filling process is repeated for the second antibonding peak. The s impurity moment and the hyperfine field increase again, they reach a maximum at Kr, then decrease, and become negative for Sr. So we see that the double-peak structure in the systematic variation of the s magnetic moment and hyperfine field of the adatoms reflects the double-peak structure of the s antibonding states in the LDOS for each spin direction, in contrast to the single-peak behavior in the bulk case.

Figure 3 shows our results for the hyperfine fields of sp impurities on the (001) surface of bcc Fe, as well

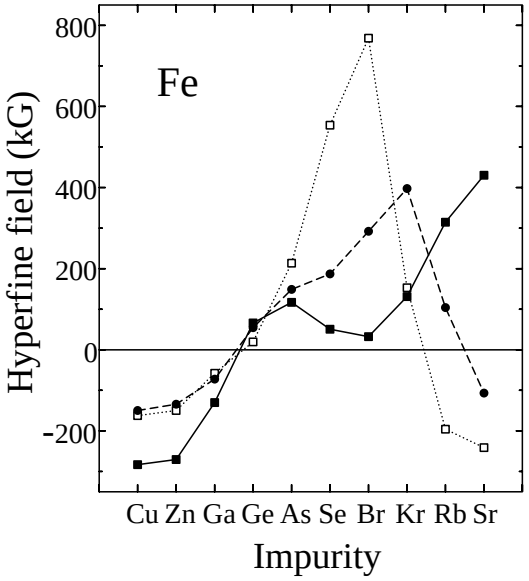

FIG. 3. Hyperfine field of sp impurities in bulk Fe (open squares, dotted line), in the first surface layer of Fe(001) (solid circles, dashed line), and adsorbed on Fe(001) (solid squares, solid line).

as in bulk Fe. For the adatoms, the first peak of the H_{hf} curve is smaller and broader than in the case of Ni, and occurs at As, while the second larger maximum is shifted to Sr. The minimum values for Se and Br and the large positive fields predicted for Rb and Sr adatoms are in striking contrast to the behavior found for the bulk impurities. Here also, the impurities in the surface layer represent an intermediate case between the bulk and adatom impurities. As can be seen by comparing the H_{hf} curves for Ni (Fig. 1) and Fe (Fig. 3), in the case of Fe all curves are shifted to higher valences. This can be explained by the stronger impurity-host hybridization, due to the larger spatial extent of the Fe d orbitals, which leads to a larger bonding-antibonding splitting. Consequently, the s antibonding states are situated higher in energy and their progressive filling, which is responsible for the systematic variation of H_{hf} as we move along within an sp series of impurities, occurs later in the case of Fe than of Ni host. Preliminary experimental results of the Berlin group [16] for Se adatoms on the Fe(001) surface yield a hyperfine field of about 40 kG, which again fits well to our calculated value of 42 kG. However, since in the experiment the Fe surface was contaminated, the close agreement could be fortuitous.

In summary, we have performed first-principles LSDA calculations using the KKR Green's function method for sp impurities on the (001) surfaces of Ni and Fe, as well as in bulk Ni and Fe. The calculated behavior for the impurity hyperfine fields of the adatoms or impurities in the first surface layer is completely different from that found in the bulk. Instead of a single maximum with very large hyperfine fields for impurities at the end of the sp series, the adatoms exhibit two maxima with a pronounced minimum in between. On Ni(001) the first maximum occurs at Ga, the second one at Kr, and small positive values are obtained for the intermediate elements Ge, As, Se, and Br. This behavior has its origin in (i) the reduced coordination number and the resulting smaller bonding-antibonding splitting of the impurity s states at the surface and (ii) the lower symmetry at the surface which leads to the formation of s-p_z hybrids on the impurity site and a doubling of the s-like bonding and antibonding peaks. As a result of the stronger hybridization on the Fe surface, both maxima are shifted to higher valences for adatoms on Fe(001). Our calculations are in very good agreement with the experiments for Se adatoms on Ni(001) and Fe(001). We hope that our results will motivate additional experiments with other probe atoms to verify the trends predicted.

We thank Dr. H. H. Bertschat for many discussions. The present work has profited from collaborations within the TMR Network "Interface Magnetism" of the European Union (Contract No. ERBFMRXCT960089) and was partially funded by the Bilateral Cooperation between Germany and Greece.

[1] G. N. Rao, Hyperfine Interact. **24-26**, 1119 (1985); M. Mohsen and F. Pleiter, Hyperfine Interact. **39**, 123 (1988).
[2] J. Kanamori, H. Katayama-Yoshida, and K. Terakura, Hyperfine Interact. **8**, 573 (1981); *ibid.* **9**, 363 (1981).
[3] M. Akai, H. Akai, and J. Kanamori, J. Phys. Soc. Jpn. **54**, 4246 (1985); *ibid.* **54**, 4257 (1985); *ibid.* **56**, 1064 (1987).
[4] S. Blügel, H. Akai, R. Zeller, and P. H. Dederichs, Phys. Rev. B **35**, 3271 (1987).
[5] H. Akai, M. Akai, S. Blügel, B. Drittler, H. Ebert, K. Terakura, R. Zeller, and P. H. Dederichs, Prog. Theor. Phys. Suppl. **101**, 11 (1990).
[6] J. Voigt, R. Fink, G. Krausch, B. Luckscheiter, R. Platzer, U. Wöhrmann, X. L. Ding, and G. Schatz, Phys. Rev. Lett. **64**, 2202 (1990).
[7] H. Granzer, H. H. Bertschat, H. Haas, W.-D. Zeitz, J. Lohmüller, and G. Schatz, Phys. Rev. Lett. **77**, 4261 (1996).
[8] B.-U. Runge, M. Dippel, G. Filleböck, K. Jacobs, U. Kohl, and G. Schatz, Phys. Rev. Lett. **79**, 3054 (1997).
[9] H. H. Bertschat, H.-H. Blaschek, H. Granzer, K. Potzger, S. Seeger, W.-D. Zeitz, H. Niehus, A. Burchard, D. Forkel-Wirth, and ISOLDE Collaboration, Phys. Rev. Lett. **80**, 2721 (1998).
[10] D. H. Rosenblatt, S. D. Kevan, J. G. Tobin, R. F. Davis, M. G. Mason, D. A. Shirley, J. C. Tang, and S. Y. Tong, Phys. Rev. B **26**, 3181 (1982); D. H. Rosenblatt, S. D. Kevan, J. G. Tobin, R. F. Davis, M. G. Mason, D. R. Denley, D. A. Shirley, Y. Huang, and S. Y. Tong, Phys. Rev. B **26**, 1812 (1982); B. Lairson, T. N. Rhodin, and W. Ho, Solid State Commun. **55**, 925 (1985).
[11] M. Mohsen and F. Pleiter, Hyperfine Interact. **39**, 123 (1988).
[12] R. Zeller, P. Lang, B. Drittler, and P. H. Dederichs, in *Application of Multiple Scattering Theory to Materials Science*, edited by W. H. Butler *et al.*, MRS Symposium Proceedings No. 253 (Materials Research Society, Pittsburg, 1992) p. 357.
[13] P. J. Braspenning, R. Zeller, A. Lodder, and P. H. Dederichs, Phys. Rev. B **29**, 703 (1984).
[14] S. H. Vosko, L. Wilk, and M. Nusair, J. Can. Phys. **58**, 1200 (1980).
[15] D. D. Koelling and B. N. Harmon, J. Phys. C **10**, 3107 (1977).
[16] H. H. Bertschat (private communication).